Synthesis and Utilization of Chiral α-Methylated α-Amino Acids with a Carboxyalkyl Side Chain in the Design of Novel Grb2-SH2 Peptide Inhibitors Free of Phosphotyrosine

Ya-Qiu Long,* Ting Xue, Yan-Li Song, Zu-Long Liu, Shao-Xu Huang, and Qiang Yu

State Key Laboratory of Drug Research, Shanghai Institute of Materia Medica, Shanghai Institutes for Biological Sciences, Chinese Academy of Sciences, 555 Zuchongzhi Road, Shanghai 201203, China

Received April 28, 2008

The growth factor receptor-bound protein 2 (Grb2) is an SH2 domain-containing docking module that represents an attractive target for anticancer therapeutic intervention. To improve the potency and bioavailability of the Grb2-SH2 inhibitors, the chiral α-methyl-α-carboxyalkyl amino acid [(α-Me)Aa] was designed to cover dual structural and functional features separately contributed by 1-aminocyclohexanecarboxylic acid (Ac6c) and α-aminoadipic acid (Adi) in position Y + 1. The enantiopure L(or D)-(α-Me)Aa bearing various chain length carboxylalkyl side chain was conveniently synthesized by an optimized oxazolidinone methodology. The incorporation of (*S*)-(α-Me)Aa into the non-pTyr-containing peptide framework with a 5-amino acid sequence binding motif of X^{-2}-Leu-(3′-substituted-Tyr)^{0} -X^{+1}-Asn really improved the inhibitory activity, affording potent (*R*)-sulfoxide-bridged cyclic and an open-chain series of pentapeptide inhibitors of Grb2-SH2 domain (IC_{50} = 1.1−5.8 μM). More significantly, these (α-Me)Aa incorporated peptide inhibitors showed excellent activities in inhibiting the growth of erbB2-dependent MDA-MB-453 tumor cell lines with low micromolar IC_{50} values, owing to the reduced peptidic nature and absence of pTyr or pTyr mimetics.

Introduction

Growth factor receptor bound protein 2 (Grb2[a]) is a ubiquitously expressed adaptor protein possessing a single Src homology 2 (SH2) domain flanked by two Src homology 3 (SH3) domains.[1] Via its SH2 domain binding to the specific phosphotyrosine(pTyr)-containing sequences on the activated growth factor receptors, Grb2 plays a crucial role in signaling from the receptor tyrosine kinases (RTK) to the Ras-MAPK cascade, serving as a bridging element between cell surface growth factor receptors and the Ras protein.[2,3] An aberrant Grb2-SH2 dependent Ras activation pathway has been described to contribute to processes important for cancer development (i.e., cell proliferation, apoptosis, and metastasis).[4−7] Thus, agents that bind to the Grb2-SH2 domain and prevent its normal function could disrupt associated PTK signaling and serve as alternatives to kinase-directed inhibitors as anticancer therapeutics.[8−11] Significant research has been devoted to enhancing binding affinity, cellular potency, and metabolic stability of Grb2-SH2 domain inhibitors that normally require an anionic phosphate-mimicking functionality for effective binding and thus potentially present membrane transport problems.[12] Our approach based on a phage library display provides a new class of Grb2-SH2 binding motif independent of phosphotyrosine, conferring better bioavailability and higher selectivity.[13−16] However, the extended peptide nature of the nonphosphorylated Grb2-SH2 inhibitor family still hinders its further development.

One efficient approach to decrease the peptidic character without loss of affinity is to create unnatural amino acid with special structural features to achieve the favored conformation and function within the pTyr binding pocket as the surrogate of several residues. It is well-known that the Grb2-SH2 domain preferentially binds to a protein or peptide ligand bearing a pY−X−N sequence in a β-turn conformation.[17,18] Therefore, the incorporation of the β-turn inducing amino acid (Figure 1) such as 1-aminocyclohexanecarboxylic acid (Ac6c)[19] or α-methylphosphotyrosine [(α-Me)pTyr] and its mimetic α-methyl-*p*-phosphonophenylalanine ((α-Me)Ppp) [20,21] in the pY + 1 position confers high affinity. However, further effort on the optimization of pY + 1 residue with tetralin-based (*S*)-2-amino-6-phosphonotetralin-2-carboxylic acid (Atc(6-PO_3H_2)), which simultaneously presents structural features of both (α-Me)Ppp and Ac6c,[22] or 4-aminopiperidine-4-carboxylic acid (Apc) derivatives, which might extend functionality outward from the Ac6c residue to an unexplored region of Grb2-SH2 protein proximal to the pTyr+1 position,[23] just turns out slight or little affinity-enhancing effect. Especially the combined residue of tetralin hybrid Atc(6-PO_3H_2) proved deleterious for the Grb2-SH2 binding when incorporated into position pY + 1 of the phosphorylated tripeptide scaffold, due in part to the rigid conformational constraint endowed to the pTyr moiety.[22]

By examination of our phage-library derived nonphosphorylated cyclic peptide ligands of Grb2-SH2 domain (termed G1TE series; examples are presented in Figure 2), the consensus sequence of YXNX also adopts β-bend type conformation facilitated by the presence of the β-turn inducing amino acid Ac6c and an *R*-configured sulfoxide cyclization linkage.[16,24] Besides, α-aminoadipic acid (Adi) as well as the Ac6c has been shown to be optimal for the Y + 1 position, with Ac6c inducing the β-bend conformation needed for binding[15,16] and Adi providing good ionic interactions with Ser141 and Arg142 residues within the binding pocket.[15,25,26] So we are intrigued to combine the two structural features of Ac6c and Adi into a

* To whom correspondence should be addressed. Phone: 86-21-50806876. Fax: +86-21-50806876. E-mail: yqlong@mail.shcnc.ac.cn.

[a] Abbreviations: Grb2, growth factor receptor-bound protein 2; SH2, src homology domain 2; Ras, rat sarcoma; MAPK, mitogen activated protein kinase; RTK, receptor tyrosine kinase; (α-Me)Aa, α-methylated amino acid; Ac6c, 1-aminocyclohexanecarboxylic acid; Adi, α-aminoadipic acid; pTyr, phosphotyrosine; Ava, ω-aminovaleric acid; Gla, γ-carboxyglutamic acid; (α-Me)Asp, α-methylaspartic acid; (α-Me)Glu, α-methylglutamic acid; (α-Me)Adi, α-methyladipic acid; 3-NH_2-Tyr, 3′-aminotyrosine; (α-Me)pTyr, α-methylphosphotyrosine; (α-Me)Ppp, α-methyl-*p*-phosphonophenylalanine; Atc(6-PO_3H_2), 2-amino-6-phosphonotetralin-2-carboxylic acid; Apc, 4-aminopiperidine-4-carboxylic acid.

10.1021/jm800487r CCC: $40.75
Published on Web 09/27/2008

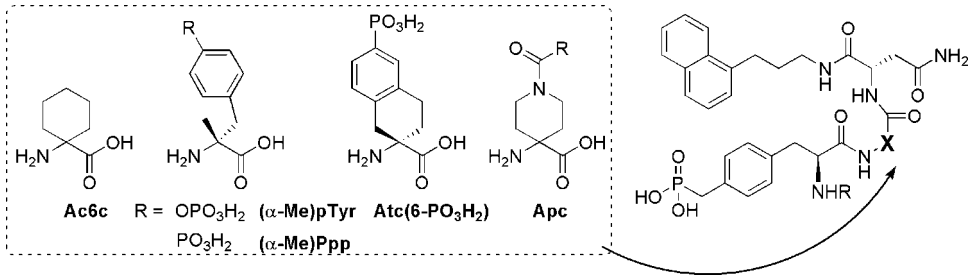

Figure 1. Structures of the β-turn inducing amino acids incorporated in pY + 1 position of the phosphopeptide inhibitor of Grb2-SH2 domain.

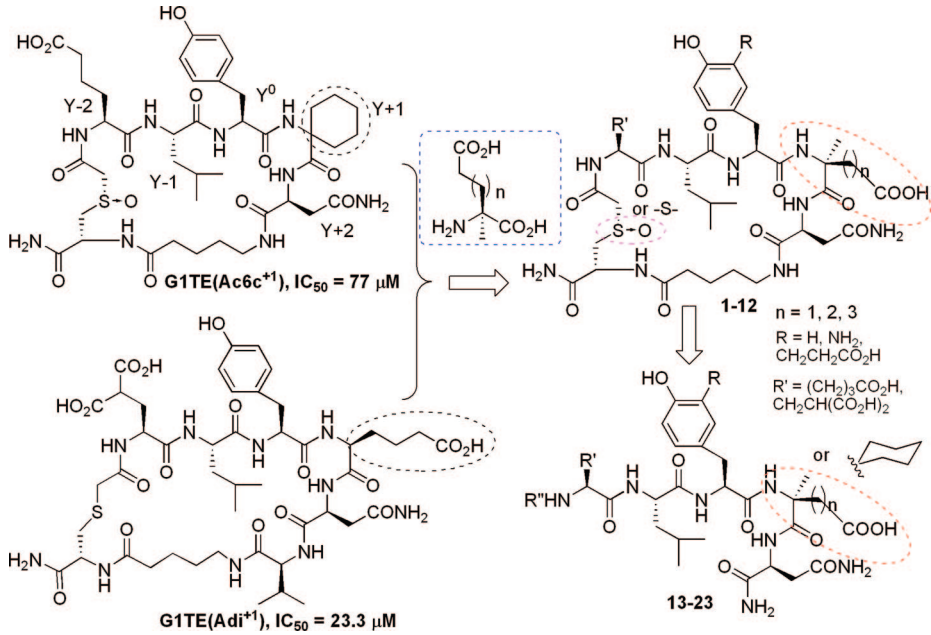

Figure 2. Design of α-methylated α-amino acids ((α-Me)Aa) bearing a carboxylic side chain to serve as a dual structural and functional building block in novel nonphosphorylated peptide ligands binding to Grb2-SH2 domain.

single residue, namely, the α-methylated α-amino acid ((α-Me)Aa) bearing various length carboxyalkyl side chain[27] (Figure 2). We suppose that this new type of hybrid chiral α,α-disubstituted amino acids could function as a dual structural and functional building block in position Y + 1 for the nonphosphorylated peptide motif binding to Grb2-SH2. On one hand, it could serve as a structural component to induce the formation of β-turn; on the other hand, the acidic functionality of its carboxyl side chain could gain potential interactions with the Grb2-SH2 domain Ser141 and Arg142 residues.[15] Noteworthy, the open chain design of the hybrid α-methyl-α-carboxyalkyl amino acid could avoid the unfavored local conformational constraint issue encountered by the tetralin-based Atc(6-PO_3H_2) within the phosphotyrosyl peptide platform.[22] This is an alternative approach in the design and structural optimization of the non-pTyr containing peptide ligands for an affinity enhancement within a simplified scaffold.

Furthermore, our group recently discovered that 3′-substituted tyrosine bearing amino or carboxylic acid group as the substituent is advantageous for the Grb2-SH2 binding because of an extensive hydrogen bonding interaction and strengthened cation−π interaction between 3′-substituted-Tyr^0 and the Arg67 and Ser88 residues within the Grb2 binding pocket.[16,28] On the basis of these observations, we applied the combination strategy further to the whole binding motif by simultaneously incorporating 3′-substituted tyrosine and chiral α,α-disubstituted amino acid in the nonphosphorylated peptide ligand, with the purpose to achieve a synergistic effect and afford potent Grb2-SH2 inhibitors with reduced charge and peptide character.

Herein, we report the synthesis and utilization of α-methylated α-amino acids with various length carboxylic acid side chains in the design of novel Grb2-SH2 inhibitors free of phosphotyrosine. In combination with the incorporation of 3′-substituted tyrosine, we designed two series of nonphosphorylated Grb2-SH2 inhibitors. As depicted in Figure 2, the (*R*)-sulfoxide-cyclized peptide comprising a 5-amino acid sequence motif, Xx^{-2}-Leu-(3′-substituted-$Tyr)^0$-(α-Me)Aa^{+1}-Asn, served as the starting scaffold to evaluate the effect of the hybrid (α-Me)Aa bearing various length carboxylic acid side chains on the Grb2-SH2 binding affinity (compounds **1**−**12**). Considering that the conformationally restricted (α-Me)Aa can induce the formation of β-turn through the local conformational constraint, we try to open the head-to-tail cyclic peptide into a linear structure (compounds **13**−**23**) with the assistance of favorable substitutions in *N*-terminus and positions Y^0 and Y + 1 for retaining effective binding. Although a previous study indicated that for the nonphosphorylated library based peptide, the cyclized constrained structure is necessary for retention of significant Grb2-SH2 binding affinity,[13,25] we expect that the introduction of the dual structural and functional residue (α-Me)Aa in combination with the presence of the optimal substitutions could make up the loss of potency as the result of the loss of global conformational constraint, thus providing a new template with

Scheme 1. Synthetic Route towards α-Methylated α-Amino Acids Bearing a Carboxylic Acid Side Chain with Various Chain Lengths Suitably Protected for Solid Phase Peptide Synthesis[27,a]

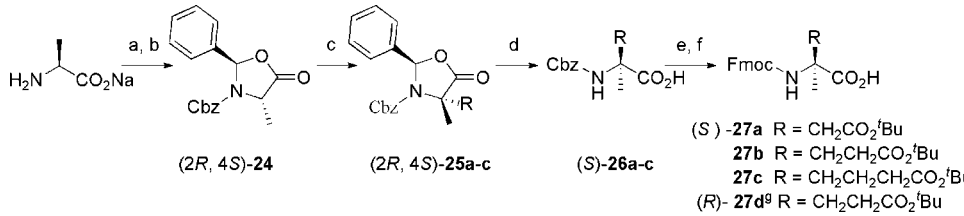

[a] Reagents and conditions: (a) benzaldehyde, DCM, reflux; (b) benzyl chloroformate, 0 °C to room temp; (c) LDA, alkyl halide, −78 °C to room temp; (d) NaOH, MeOH/H_2O (1/1); (e) H_2, 10% Pd−C, MeOH; (f) FmocOSu, 10% Na_2CO_3/dioxone; (g) starting from D-alanine employing the same procedure to give (*R*)-α-methylglutamic acid.

Scheme 2. Optimized Synthetic Route toward α-Methylaminoadipic Acid δ-(*tert*-Butyl ester)[a]

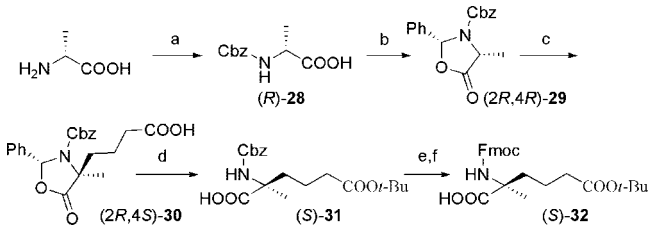

[a] Reagents and conditions: (a) $PhCH_2OCOCl$, NaOH (2 N), 0 °C; (b) $PhCH(OMe)_2$, $BF_3 \cdot Et_2O$, −40°C, 4 days; (c) *tert*-butyl 4-iodobutanoate, LiHMDS, THF/HMPA = 4: 1, −78°C; (d) $LiOH \cdot H_2O$, THF/H_2O = 3: 1, 0 °C; (e) H_2, Pd/C, MeOH; (f) FomcOSu, Na_2CO_3, acetone/H_2O = 1:1.

simplified structure for the development of potent and druglike Grb2-SH2 inhibitors.

Synthesis

We designed a series of α-methylated α-amino acids with various chain length of carboxyalkyl side chains to determine the optimal distance of the carboxylic acid functionality in the interaction with the Grb2-SH2 binding pocket. Efficient approaches have been developed to synthesize the chiral α,α-disubstituted amino acids in protected forms bearing carboxy-*tert*-butyl protection in the side chain and *N*-α-Fmoc protection at the backbone suitable for solid phase peptide synthesis using the Fmoc protocol, as depicted in Schemes 1 and 2.

Basically, the synthesis of the unnatural (α-Me)Aa is based on the literature-reported oxazolidinone methods,[27,29] but the synthetic strategy of the key intermediate, i.e., 2-phenyl-3-carbobenzyloxyoxazolidinone, is different between the two approaches, which resulted in different chiral induction effects. The concerted cyclization and *N*-Cbz protection of oxazolidinone approach affords the *trans*-2-phenyl-4-methyloxazolidinone (Scheme 1), whereas the sequential *N*-Cbz protection and cyclization approach generates predominantly *cis*-2-phenyl-4-methyloxazolidinone (Scheme 2). We modified the latter methodology for the synthesis of α-methyladipic acid bearing a long hydrocarbon side chain, which was produced in poor yield by the literature-reported methods.

General Synthesis toward the α-Methyl-Substituted α-Amino Acids Bearing Carboxyalkyl Side Chains with Various Chain Length.[27] As shown in Scheme 1, the starting material L-alanine was converted to the Schiff base with benzaldehyde followed by cyclization to the oxazolidinone (2*R*,4*S*)-**24** by addition of benzyl chloroformate. Alkylation of (2*R*,4*S*)-**24** was performed with lithium diisopropylamide (LDA) as base and alkyl halide as electrophile to give 4-disubstituted oxazolidinone (2*R*,4*S*)-**25**. The alkylation reaction proceeded with excellent stereoselectivity with attack of the electrophile from the face opposite to the phenyl group. Then the base-promoted ring opening of the oxazolidinone (2*R*,4*S*)-**25** led to protected amino acid derivative (*S*)-**26**, which was carried out with NaOH in MeOH/H_2O mixtures. Hydrogenation followed by treatment with FomcOSu furnished the desired compound (*S*)-**27**, suitably protected for solid-phase peptide synthesis. The corresponding enantiomer, i.e., (*R*)-**27**, can be synthesized starting from D-alanine using the same procedure.

However, when applied to the synthesis of α-methylaminoadipic acid δ-(*tert*-butyl ester), this method failed to give satisfying yield. So we switched to S. Karady's method, which involved the conversion of the amino acid to the *cis*-2-aryl-3-carbobenzyloxyoxazolidinone followed by the enantioretentive alkylation of the potassium enolate.[29]

Optimized Synthetic Route toward α-Methylaminoadipic Acid *δ*-(*tert*-Butyl ester). As shown in Scheme 2, the condensation of N^{α}-Cbz-D-alanine with benzaldehyde under acidic conditions yielded predominantly *cis*-oxazolidinone, which subsequently underwent the enantioretentive alkylation under the basic conditions. The resultant 2-phenyl-4-methyl-substituted oxazolidinone underwent hydrolysis and hydrogenolysis to afford the desired product **32**.[29] Application of the Lewis acid $BF_3 \cdot Et_2O$ and the benzaldehyde dimethyl acetal in the condensation step was our modification to prepare *cis*-(2*R*,4*R*)-2-phenyl-4-methyloxazolidinone **29** in good yield. Alkylation of **29** with *tert*-butyl 4-iodobutanoate proceeded with a reasonable yield using LiHMDS as the base, yielding a single diastereomer (2*R*,4*S*)-2-phenyl-4-methyl-4-carboxyalkyloxazolidinone **30**. The alkyl group entered from the side opposite to the aryl function, which resulted in retention of the original configuration for the cis isomers.[29] The base-catalyzed opening of the oxazolidinone **30** with LiOH in THF/H_2O mixture led to the N^{α}-Cbz-protected α,α-disubstituted amino acid **31**. Hydrogenation followed by treatment with FomcOSu afforded the desired compound (*S*)-**32** with orthogonal protection suitable for solid-phase peptide synthesis based on Fmoc chemistry. The enantiomer (*R*)-**32** can be obtained from Cbz-L-Ala-OH employing the same procedure.

Cyclopeptide Synthesis. The thioether- or (*R*)-sulfoxide-bridged cyclic pentapeptide served as the template for the incorporation of the α-methyl-α-alkylcarboxylic acid amino acids with global protections. The synthesis of these thioether- or sulfoxide-bridged cyclicpeptides **1**−**12** was carried out in a manner similar to that reported previously (Scheme 3).[25] The ω-aminovaleric acid (Ava) served as a linker to maintain the global conformation and the proper orientation of the key residues in the shortened cyclic protocol.[25]

Results and Discussion

Since reducing peptidic character is an important issue in the development of Grb2-SH2 domain inhibitors as chemothera-

Scheme 3. General Synthetic Route for Thioether- and Sulfoxide-Bridged Cyclic Peptides **1**−**12**

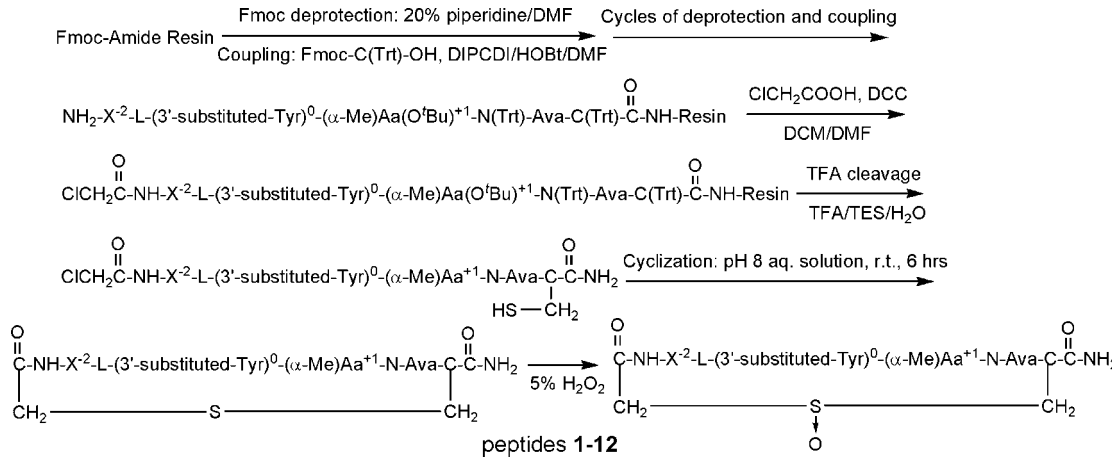

peutic agents, we proposed a new concept of dual functional and structural residue to simplify the non-pTyr containing cyclic peptide scaffold with retention of high affinity binding. The objective of the current work was to examine the Grb2-SH2 domain binding effect of the nonphosphorylated peptide family incurred by (1) the incorporation of the α-methylated α-amino acids with various length carboxylic acid side chains in the Y + 1 position within the consensus sequence of the non-pTyr containing peptide ligand and (2) opening the cyclic structure with the simultaneous insertion of the *β*-turn inducing amino acid, i.e., (α-Me)Aa or Ac6c and the favorable functional residues such as 3′-substituted Tyr and *γ*-carboxyglutamic acid (Gla).

The chain length of the side chain carrying the terminal carboxylic acid functionality within the α-methylated α-amino acids was investigated. The previously reported pentapeptide platform bearing the five amino acid long sequence of Adi-L-Y-(α-Me)Aa-N served as the starting point to determine the optimal chain length and orientation of the α-alkylcarboxylic acid side chain (**1**−**12**). In combination with the favorable substitutions of 3′-substituted Tyr and Gla in positions Y and Y − 2 within the non-pTyr containing Grb2-SH2 binding platform, we further explored an open-chain peptide inhibitor series just bearing five to three residues free of pTyr or pTyr mimetics (**13**−**23**), aimed to provide new scaffold with reduced peptidic character and reduced charge but improved potency for further chemical elaboration.

(*S*)-α-Methyladipic acid is favored in position Y + 1, and the simultaneous incorporation of 3′-aminotyrosine greatly facilitates the Grb2-SH2 binding. As expected, the incorporation of the α-methylaspartic acid ((α-Me)Asp) in replacement of Ac6c in position Y + 1 within the cyclic pentapeptide platform resulted in a 2.5-fold enhancement in potency (**2**, IC_{50} = 30 *μ*M) relative to the parent peptide G1TE(Ac6c^{+1}) (IC_{50} = 77 *μ*M), as shown in Table 1. The positive result supported our hypothesis to some extent that the α-methyl-α-carboxyalkyl amino acid could function as the dual residue to display both the *β*-turn inducing effect and side chain functionality potentiating effect. Consistent with previous findings, the thioether-cyclized peptide **1** with (α-Me)Asp^{+1} substitution (**1**, IC_{50} = 108 *μ*M) was less potent than the *R*-configured sulfoxide-cyclized analogue **2**. Extending the carboxyl side chain of (α-Me)Asp by one methylene unit (X^{+1} = (α-Me)Glu) gained a further improvement of the binding affinity by 1.5- to 1.7-fold (IC_{50} = 70 *μ*M for thioether-bridged peptide **3**; IC_{50} = 18 *μ*M for (*R*)-sulfoxide-bridged peptide **4**), probably due to the more flexible side chain capable of positioning the carboxyl functionality properly in the binding pocket. However, addition of one more methylene unit on the carboxyl side chain (X^{+1} = (α-Me)Adi) did not increase the activity proportionally. The inhibitory activity of (α-Me)Adi^{+1} containing cyclic peptides **5** (IC_{50} = 61 *μ*M) and **6** (IC_{50} = 17 *μ*M) was slightly more potent than that of peptides **3** and **4**, respectively, indicating that (α-Me)Glu and (α-Me)Adi make almost equal contribution to the peptide interaction with the Grb2-SH2 domain when located in position Y + 1.

Since the chiral α,α-disubstituted amino acid involves the stereo orientation of the side chain, it is of interest to examine the reversed configuration of the α-methylated α-amino acid residue. However, when the side chain was reversely orientated, the enantiomer (*R*)-(α-Me)Glu containing peptide suffered a loss of binding affinity (**7**, IC_{50} = 60 *μ*M; **8**, IC_{50} = 30 *μ*M) compared to the (*S*)-(α-Me)Glu containing congeners, probably

Table 1. Grb2-SH2 Binding Affinity of Cyclic Pentapeptide Containing α-Methylated Amino Acid in Position Y + 1[a]

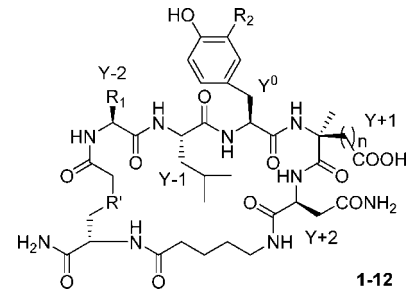

1-12

compd	R_1	R_2	*n*	R′	IC_{50} (*μ*M)[b]
G1TEp (Ac6c^{+1})	$CH_2(CH_2)_2COOH$	H		(*R*)-S=O	77[c]
1	$CH_2(CH_2)_2COOH$	H	1	S	108 ± 2.5
2	$CH_2(CH_2)_2COOH$	H	1	(*R*)-S=O	30.5 ± 4.5
3	$CH_2(CH_2)_2COOH$	H	2	S	70 ± 3.5
4	$CH_2(CH_2)_2COOH$	H	2	(*R*)-S=O	18 ± 4.0
5	$CH_2(CH_2)_2COOH$	H	3	S	60.7 ± 0.2
6	$CH_2(CH_2)_2COOH$	H	3	(*R*)-S=O	17 ± 2
7	$CH_2(CH_2)_2COOH$	H	2, (*R*)-	S	60.5 ± 0.5
8	$CH_2(CH_2)_2COOH$	H	2, (*R*)-	(*R*)-S=O	30.5 ± 6.5
9	$CH_2(CH_2)_2COOH$	NH_2	2	S	17 ± 2.5
10	$CH_2(CH_2)_2COOH$	NH_2	2	(*R*)-S=O	8.1 ± 1.0
11	$CH_2CH(COOH)_2$	NH_2	3	S	9.5 ± 1.5
12	$CH_2CH(COOH)_2$	NH_2	3	(*R*)-S=O	1.15 ± 0.05

[a] The binding assay was performed on a BIAcore 3000 instrument with the method described in the Experimental Section. [b] Values are the mean of at least two independent experiments and are expressed as the concentration at which half-maximal competition was observed (IC_{50}). Standard deviation is given in parentheses. [c] The binding data was cited from ref 16.

because the carboxyl functionality failed to reach the proper site for interaction with the binding pocket. Therefore, the *S*-configured α-methylated α-amino acid was preferable in position Y + 1 over the *R*-configured one in the context of the nonphosphorylated peptide ligand binding to Grb2-SH2 protein.

Interestingly, although the affinity-enhancing effect of the hybrid (α-Me)Aa was not as great as we expected, the combination of 3′-aminotyrosine (3′-NH_2-Tyr) substituted in position Y^0 and γ-carboxyglutamic acid (Gla) in position Y − 2 significantly boosted the binding affinity (Table 1, entry **9**−**12**). As our previous study has revealed, the Gla^{-2} carboxyl groups together with Tyr^0 interact with Arg67 (αA-helix) and Arg86 (βC-strand) residues and the three Ser residues 88, 90, and 96 within the binding pocket, compensating for the absence of Tyr^0 phosphorylation in maintaining effective binding to the Grb2-SH2 domain.[14−16] Correspondingly, the replacement of Tyr with 3-NH_2-Tyr resulted in a dramatic enhancement of the potency, due in part to a strengthened cation−π interaction between the electron-rich phenol ring of Tyr and the electron-deficient Arg67 side chain of the Grb2 SH2 domain binding cavity.[16,30] Undoubtedly, the incorporation of 3-NH_2-Tyr^0 into (α-Me)Glu^{+1} containing thioether-cyclized pentapeptide afforded a 4-fold improvement in the activity (peptide **9**, IC_{50} = 17 μM) relative to its parent peptide **2** (IC_{50} = 70 μM). And the corresponding (*R*)-sulfoxide cyclized analogue is 2-fold more potent (**10**, IC_{50} = 8.1 μM).

Considering the synergetic effect of the combined substitutions, further optimization employed all favorable structural features in the non-Tyr containing platform. Not surprisingly, the simultaneous utilization of Gla in Y − 2 position, 3-NH_2-Tyr in Y^0 position, and (α-Me)Adi in Y + 1 position of the (*R*)-sulfoxide-bridged cyclic pentapeptide resulted in a significant enhancement of the Grb2-SH2 domain binding affinity (**12**, IC_{50} = 1.15 μM), which is 8-fold more potent than its thioether precursor (**11**, IC_{50} = 9.5 μM) and 66-fold more potent than the parent peptide G1TE($Ac6c^{+1}$) (IC_{50} = 77 μM), encouraging us to try an open chain nonphosphorylated Grb2-SH2 inhibitor with the assistance of the beneficial structural and functional residues to retain significant binding.

Combination of beneficial structural modifications with (α-Me)Adi, 3′-NH_2-Tyr, and Ac6c affords an open chain peptide scaffold significantly binding to Grb2-SH2 domain free of pTyr or pTyr mimics. Decreasing the peptidic character and simplifying the macrocycle structure have been an important issue in the development of Grb2-SH2 domain inhibitors as chemotherapeutic agents. Considering that the conformationally restricted (α-Me)Aa can induce the turn-geometry through the local conformational constraint, we are intrigued to delete the auxiliary linker of G1TE family to afford an open-chain peptide scaffold. Although a previous study indicated that for the nonphosphorylated library based peptide, the cyclized constrained structure is necessary for maintenance of high affinity Grb2-SH2 binding,[13,25] it was hoped that the introduction of the dual structural and functional residue (α-Me)Aa combined with the optimal substitutions could make up the loss of potency as a result of the loss of global conformational constraint, thus providing new template with simplified structure for the development of potent and druglike Grb2-SH2 inhibitors.

As shown in Table 2, the adverse effect caused by the deletion of the Ava linker and the thioether/(*R*)-sulfoxide bridge was indeed offset by the presence of Gla^{-2}, 3-NH_2-Tyr^0, and (α-Me)Glu^{+1}. The resulting open-chain pentapeptide **13** exhibited an equipotent binding affinity (IC_{50} = 19 μM) as the original lead peptide G1TE, a thioether-cyclized decapeptide with the sequence of ELYENVGMYC.[13,14] Furthermore, the attachment of an Fmoc group on the N-terminus of peptide **13** harvested a low-micromolar affinity peptide inhibitor of Grb2-SH2 domain (**14**, IC_{50} = 4.4 μM) devoid of any pTyr or pTyr mimics and macrocyclization. Concerning the N-terminal modification, it was literaturely reported that an anthranyl moiety to the N-terminus of phosphopeptide H-Glu-pTyr-Ile-Asn-NH_2 produced a dramatic increase of binding affinity for the Grb2-SH2 protein,[31] originating from an efficient π−cation stacking between the electron-rich anthranyl ring of the phosphopeptide and the electron-deficient guanidinium group of Arg αA2 residue within the pTyr binding pocket.[32] Another 3-aminobenzyloxycarbonyl group was observed to confer a similar potentiating effect when attached to the N-terminus of phosphopeptide H-pTyr-Ile-Asn-NH_2 via the same mechanism.[31] So we propose that the affinity-enhancing effect of Fmoc on the N-terminus of open chain nonphosphopeptide might be attributed to the π−cation interaction of the 9*H*-fluorene ring with the Arg αA2 guanidinium group.

Table 2. GRB2-SH2 Binding Affinity of Open Chain Small Peptide Containing α-Methylated Amino Acid in Position Y + 1

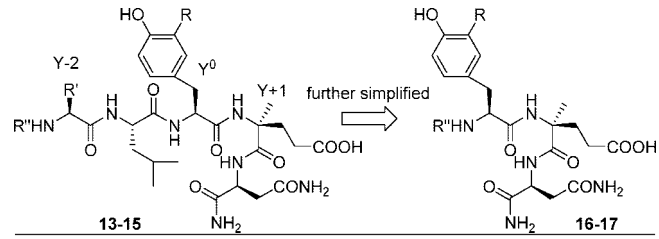

compd	R	R′	R″	IC_{50} (μM)
13	NH_2	$CH_2CH(COOH)_2$	H	19 ± 2.4
14	NH_2	$CH_2CH(COOH)_2$	Fmoc	4.4 ± 1.2
15	$CH_2CH_2CO_2H$	$CH_2(CH_2)_2COOH$	Fmoc	5.6 ± 1.9
16	$CH_2CH_2CO_2H$	deleted	H	290 ± 84
17	$CH_2CH_2CO_2H$	deleted	Fmoc	168 ± 51

With the help of Fmoc on the N-terminus, the replacement of 3′-NH_2-Tyr^0 with 3′-carboxyethyl-Tyr and substitution of Gla^{-2} with Adi in peptide **14** still secured an effective binding to Grb2-SH2 (peptide **15**, IC_{50} = 5.6 μM). Of note, the 3′-carboxyethyl-Tyr was developed as a new type of pTyr mimetic in our group and exhibited a potentiating effect in the cyclic non-phosphopeptide ligand family because of an enhanced electrostatic interaction between the 3′-carboxy group of the tyrosine and the pTyr binding pocket.[28] In the context of the open-chain non-pTyr containing peptide, the combination of 3′-carboxyethyl-Tyr in position Y^0 and Adi in position Y − 2 works as well.

Since the acidic side chain of Adi^{-2} shared an overlapping function with the Tyr^0, the carboxyl functionality of the 3′-carboxyethyl-Tyr in position Y^0 might partially take over the role of the carboxyl group in position Y − 2 in turn. Hence in further development, the residues in positions Y − 2 and Y − 1 were deleted in the presence of 3′-carboxyethyl-Tyr^0 to determine the minimal binding sequence within the open-chain non-phosphopeptide ligand of Grb2-SH2 domain. Disappointingly, the removal of residues Adi^{-2} and Leu^{-1} resulted in a big but not complete loss of the activity (peptide **16**, IC_{50} = 290 μM), indicating that the idea of 3′-carboxyethyl-Tyr^0 compensating for the absence of Adi^{-2} was plausible. Additional introduction of a Fmoc group in the N-terminus of the tripeptide just increased the affinity by a factor of 1.7-fold (peptide **17**, IC_{50} = 168 μM). Obviously, the acidic residue in position Y − 2 did play an important role in the binding of the non-pTyr containing peptide with the Grb2-SH2 protein. Meanwhile, the

Table 3. Grb2-SH2 Binding Affinity of Open Chain Pentapeptide Incorporated α-Methylated Amino Acid in Position Y − 2 and 1-Aminocyclohexanecarboxylic Acid (Ac6c) in Position Y + 1

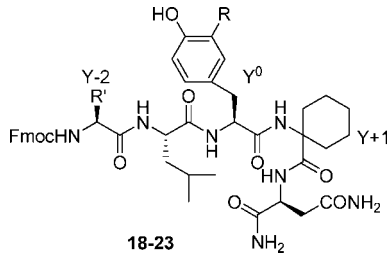

18-23

compd	R	R′	IC_{50} (μM)
18	NH_2	Adi	5.8 ± 1.8
19	NH_2	Gla	2.5 ± 1.1
20	H	(*R*)-(α-Me)Adi	>1000
21	H	(*S*)-(α-Me)Adi	117.7 ± 20
22	NH_2	(*R*)-(α-Me)Adi	700 ± 68
23	NH_2	(*S*)-(α-Me)Adi	3.9 ± 1.0

spatial arrangement of the carboxylic functionality in position Y − 2 is also an important issue, with the desired orientation being pointed to the same direction as the side chain of Tyr^0 to accomplish the compensatory action.

Taking the orientation issue into account, we modified our open-chain pentapeptide platform by locating the conformationally restricted α-methyl-α-carboxyalkyl amino acid in the Y − 2 position and another turn-inducing element Ac6c in the Y + 1 position instead. It was anticipated that the local conformational constraint of the (α-Me)Aa could limit the side chain mobility to preserve the optimal orientation of the carboxyl group. Thereafter, further structural optimization was carried out on the new template (Table 3).

As shown in Table 3, the replacement with Ac6c in position Y + 1 maintained binding affinity nearly equal to that of the parent (α-Me)Glu residue in the open chain sequence of Fmoc-Xx^{-2}-L-(3′-NH_2-Tyr)-Xx^{+1}-N, indicating that Ac6c is really an optimal residue for the Y + 1 position with its ability to induce the β-bend conformation and to afford van der Waals interactions with Phe βD5 and Gln βD3.[33] Thereby, the introduction of the well-known beneficial structural modification with Adi or Gla in position Y − 2 certainly produced high affinity linear non-pTyr containing peptides **18** (IC_{50} = 5.8 μM) and **19** (IC_{50} = 2.5 μM), with Gla being more favored than Adi, affording the highest Grb2-SH2 binding affinity in this open-chain non-Tyr-containing peptide series.

It is of note that the Ac6c exhibited a more potent potentiating effect in position Y + 1 than (α-Me)Glu in the context of conformationally unrestricted open-chain peptide series, indicated by the inhibitory activity difference of (α-Me)Glu^{+1} containing peptide (**14**, IC_{50} = 4.4 μM) and the $Ac6c^{+1}$ containing counterpart peptide (**19**, IC_{50} = 2.5 μM). We assumed that the local conformational constraint endowed by the Y + 1 residue plays a critical role in the Grb2-SH2 binding in the absence of the global conformational restriction. In this regard, the cyclic rigid Ac6c is more beneficial for inducing the required β-turn conformation of the open-chain peptide than the linear flexible residue (α-Me)Glu. The calculation of the angle between the α,α-disubstituted groups by using SYBYL package software (*Version* 6.8, Tripos Associates, St. Louis, MO, 2000) confirmed our assumption. The angle of Ac6c is 108.98 degree, and that of (α-Me)Glu is 112.22 degree. Nevertheless, the chiral (α-Me)Aa residue involved the spatial arrangement issue, which showed the benefit to position the acidic group into proper site in the binding to Grb2-SH2 protein.

As far as the orientation is concerned, the configuration of the (α-Me)Adi in position Y − 2 was investigated to determine the optimal spatial arrangement. The introduction of (*R*)-(α-Me)Adi^{-2} into the general template Fmoc-Xx^{-2}-Leu-Tyr-$Ac6c^{+1}$-Asn almost abolished the activity (**20**, IC_{50} > 1000 μM), while the enantiomeric (*S*)-(α-Me)Adi^{-2} prominently improved binding affinity (**21**, IC_{50} = 117 μM), suggesting that (*S*)-configured α-methyl-α-carboxyalkyl amino acid might position the carboxyalkyl side chain to the desired site capable of overlapping with the phenol functionality of Tyr^0. Consistently, combining the (*S*)-(α-Me)Adi^{-2} substitution with another beneficial structure of 3′-NH_2-Tyr in replacement of Tyr^0 resulted in a high affinity linear peptide inhibitor of Grb2-SH2 (**23**, IC_{50} = 3.9 μM), which is 30 times more potent than the parent compound **21**. As a comparison, the substitution of the reversed configuration (*R*)-(α-Me)Adi^{-2} did impair the inhibitory activity (**22**, IC_{50} = 700 μM), confirming that the (*S*)-configuration α-methyl-α-carboxyalkyl amino acid is suitable for driving the carboxyl side chain in proximity to the 3′-NH_2-Tyr^0 side chain. Comparison of peptide **18** with peptide **23** clearly demonstrated that the conformationally constrained α-methyladipic acid was advantageous in the position Y − 2 over α-adipic acid. The local conformational constraint did help the carboxylic acid functionality orientate toward the pTyr binding pocket as we anticipated.

Antiproliferative Effects in Breast Cancer Cells in Culture. The utilization of the hybrid residue reduced the molecular size and charge of the non-pTyr containing Grb2-SH2 inhibitors with retention of high affinity binding; thus, the cellular potency was expected to be improved accordingly. Therefore, cell proliferation assays were conducted to evaluate the effectiveness of our synthetic peptides to inhibit the intracellular association of native Grb2 protein with activated cellular growth factor receptor. MDA-MB-453 breast cancer cell line was used, which overexpresses erbB-2,[4] mitogenically driven through Grb2-dependent signaling pathways. The potent (*S*)-(α-Me)Adi containing cyclic and linear Grb2-SH2 inhibitors (peptides **12**, **14**, **15**, **19**, and **23**) were selected for this purpose. Very encouragingly, these peptides displayed moderate to potent antiproliferative effects against the MDA-MB-453 cells with the cyclic peptide **12** (IC_{50} = 12 μM) being the most potent (Figure 3), which indicated that these peptides with reduced charge and peptidic character were able to penetrate the cell membrane and effectively block erbB-2-driven growth in breast cancer cells. Comparison of the cellular potency of peptides **19** (IC_{50} = 52 μM) and **23** (IC_{50} = 29 μM) suggested that (α-Me)Adi is more favorable in position Y − 2 over Gla in the cellular context, since the former possessed less carboxylic acid group. The same is true for peptide **14** which bore the double-charged Gla in position Y − 2, thus impairing the cellular activity (IC_{50} = 55 μM).

Conclusions

In this study, we proposed a new concept by combining the structural features of Ac6c and Adi into a single residue, namely, a dual structural and functional residue. Previous SAR studies have revealed that Ac6c and Adi are optimal Y + 1 residues for high affinity Grb2-SH2 domain binding of the nonphosphorylated peptide family, with Ac6c inducing the β-turn conformation needed for binding and Adi providing good ionic interactions with Ser141 and Arg142 residues within the binding pocket. Thus, the designed hybrid α-methyl-α-carboxyalkyl amino acid was expected to play the dual role. On the simplified sulfoxide-cyclized peptide platform with a five amino acid

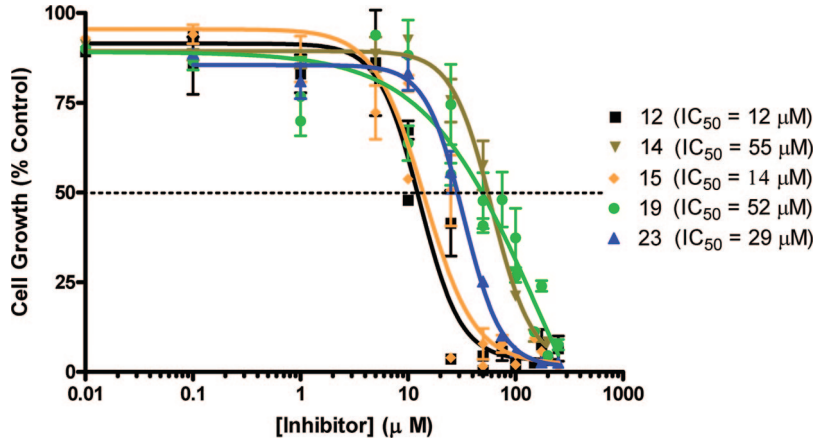

Figure 3. Inhibition of cell growth by selected peptide inhibitors of Grb2 SH2 in MDA-MB-453 breast cancer cells as determined using a WST-based assay.

sequence Adi^{-2}-Leu-Tyr^{0}-(α-Me)Aa $^{+1}$-Asn, the incorporation of (α-Me)Aa bearing various length carboxyalkyl side chains into the Y + 1 position really improved the inhibitory activity, with (α-Me)Adi being a preferable Y + 1 residue. The highest affinity was achieved by the simultaneous substitution of Gla in Y − 2 position, 3-NH_2-Tyr in Y^0 position, and (α-Me)Adi in Y + 1 position of the (*R*)-sulfoxide-bridged cyclic pentapeptide with an IC_{50} value of 1.15 μM, free of any pTyr or pTyr mimetics. Encouragingly, with the potentiating effect of the hybrid residue (α-Me)Aa, an open-chain peptide series was developed to decrease the peptidic nature and molecular size without loss of affinity. The local conformational constraint conferred by (α-Me)Aa in combination with beneficial structural modifications of Gla^{-2} and 3′-NH_2-Tyr^0 compensates for the loss of activity caused by the removal of the Ava linker and the global conformational constraint, resulting in low micromolar open-chain pentapeptide inhibitors of Grb2-SH2 domain (IC_{50} = 4.4−5.6 μM). Further development was advanced by the relocation of (*S*)-α-methyladipic acid into position Y − 2 and replacement with Ac6c in position Y + 1, affording potent open-chain pentapeptide inhibitors of the Grb2-SH2 domain with reduced charge and peptidic character (IC_{50} = 2.5−5.8 μM). Interestingly, the (α-Me)Aa containing cyclic and linear peptides exhibited excellent antiproliferative activity against erbB-2-dependent MDA-MB-453 breast cancer cells. The first utilization of the dual structural and functional residue, namely, chiral α-methyl-α-carboxyalkyl amino acid, created a new class of high affinity open-chain nonphosphorylated peptide inhibitors of Grb2-SH2 domain and potentially may find value in chemical therapeutics for erbB2-related cancers.

Experimental Section

Binding Affinity Measurements Using Surface Plasmon Resonance (SPR) Analysis. The competitive binding affinity of ligands for the Grb2-SH2 protein was assessed using Biacore SPR methods on a BIAcore 3000 instrument (Pharmacia Biosensor, Uppsala, Sweden). IC_{50} values were determined by mixing the inhibitor with recombinant Grb2 SH2 protein and measuring the amount of binding at equilibrium to an immobilized SHC (pTyr-317) phosphopeptide, i.e., biotinyl-DDPS-pY-VNVQ, in a manner similar to that reported previously.[13] Briefly, the biotinylated phosphopeptide was attached to a streptavidin coated SA5 biosensor chip, and the binding assays were conducted in pH 7.4 PBS buffer containing 0.01% P-20 surfactant (Pharmacia Biosensor).

Examination of Antiproliferative Effects of Synthetic Inhibitors against Breast Cancer Cells in Culture. MDA-MB-453 cells were seeded in 96-well flat bottom cell culture plates at a density of (3−4) × 10^3 cells/well with synthetic inhibitors and incubated for 4 days. Cell growth inhibition after treatment with the various concentrations of the inhibitors was determined by WST-8 (2-(2-methoxy-4-nitrophenyl)-3-(4-nitrophenyl)-5-(2,4-disulfophenyl)-2*H*-tetrazolium monosodium salt (Dojindo Molecular Technologies Inc., Gaithersburg, MD). WST-8 was added at a final concentration of 10% to each well, and then the plates were incubated at 37 °C for 2−3 h. The absorbance of the samples was measured at 450 nm using a TECAN ULTRA reader. Concentration of the peptides that inhibited cell growth by 50% (IC_{50}) was calculated by comparing absorbance in the untreated cells (DMSO control) and the cells treated with the varying concentrations of inhibitors.

General Synthetic Procedures. ^{1}H NMR spectra were recorded on a Varian Mercury 300 or 400 MHz spectrometer. The data are reported in parts per million relative to TMS and referenced to the solvent in which they were run. Elemental analyses were obtained using Vario EL spectrometer. Melting points (uncorrected) were determined on a Buchi-510 capillary apparatus. EI-MS spectra were obtained on a Finnigan MAT 95 mass spectrometer, and ESI-MS spectra were recorded on a Finnigan LCQ Deca mass spectrometer. Liquid chromatography−mass spectrometry (LC−MS) was carried out on Waters Micromass ZQ2000. Specific rotations (uncorrected) were determined in a Perkin-Elmer 341 polarimeter. The solvent was removed by rotary evaporation under reduced pressure, and flash column chromatography was performed on silica gel H (10−40 μm). Anhydrous solvents were obtained by redistillation over sodium wire.

All peptides were synthesized manually using standard solid phase peptide chemistry with Fmoc protected amino acids on Pal resin at a 0.1 mmol scale. Couplings with Fmoc amino acids (2.5 equiv) were performed in the presence of 1-hydroxybenzotriazole (HOBT) and 1,3-diisopropylcarbodiimide (DIPCDI) (each 2.5 equiv) in DMF (5 mL) at room temperature for 2 h, and then the Fmoc protecting group was removed by treatment with 20% piperidine in DMF (5 mL) at room temperature for 20 min. The syntheses of the thioether- and sulfoxide-bridged cyclic peptides were similar to the procedure described previously.[18,20] The final product was purified by semipreparative reverse phase HPLC. RP-HPLC conditions are as follows: Vydac C18 column (20 mm × 250 mm); solvent gradient system 1, (A) 0.05% TFA in water, (B) 0.05% TFA in 90% acetonitrile in water; solvent gradient system 2, (A) 0.05% TFA in water, (C) 0.05% TFA in 90% methanol in water with gradient indicated below; flow rate, 2.5 mL/min; UV detector, 225 nm. ESI-MS was performed on a Finnigan LCQ Deca mass spectrometer. The purity of products was characterized by analytical HPLC and ESI-MS. HPLC used two solvent systems: method 1, gradient 10−70% B over 30 min; method 2, gradient 10−70% C over 30 min.

(2*R*,4*S*)-3-[(Benzyloxy)carbonyl]-4-methyl-2-phenyl-1,3-oxoazolidin-5-one ((2*R*,4*S*)-24). To a suspension of sodium L-alaninate (12.5 g, 0.112 mol) in dry CH_2Cl_2 (500 mL), benzaldehyde (11.31 mL, 0.112 mol) was added, and the mixture was refluxed using a Dean−Stark apparatus for 21 h. It was then cooled to 0 °C, benzyl chloroformate (14 mL, 0.110 mol) was added, and stirring was continued at 0 °C for 5 h and then overnight at 25 °C. The crude product was dried under high vacuum. Separation of the two isomers was subsequently achieved by crystallization from $(i\text{-Pr})_2O$ at −18 °C, yielding 9.8 g (30.5%) of pure *trans*-oxazolidinone (2*R*,4*S*)-**24**. ^{1}H NMR ($CDCl_3$, 300 MHz): δ ppm 7.41−7.27 (m, 10H), 6.64 (s, 1H), 5.12 (s, 2H), 4.50 (q, 1H, J = 6.9 Hz), 1.69 (d, 3H, J = 6.9 Hz). $[\alpha]_D^{23}$ +84 (*c* 1, CH_2Cl_2).

(2*R*,4*S*)-3-[(Benzyloxy)carbonyl]-4-{[(*tert*-butyloxy)carbony]-methyl-2-phenyl-1,3-oxoazolidin-5-one ((2*R*,4*S*)-25a). LDA (10 mmol) was added to a precooled (−78 °C) solution of 7.5 mmol of (2*R*,4*S*)-**24** in 40 mL of THF. The slightly yellow enolate solution was stirred for 5−10 min at −78 °C, and then an amount of 9 mmol of alkyl halide was added. The mixture was stirred for 3 h at −78 °C and then allowed to warm to room temperature overnight. THF was evaporated, the residue portioned between saturated aqueous NH_4Cl solution and Et_2O, the aqueous layer separated and extracted twice with Et_2O, and the combined ether extracts were dried over Na_2SO_4 and evaporated to give the crude product. FC (PE/EtOAc = 10 /1) of the crude product afforded (2*R*,4*S*)-**25a** as yellow oil in a yield of 76%. ^{1}H NMR ($CDCl_3$, 300 MHz): δ ppm 7.40−7.27 (m, 10H), 6.64 (s, 1H), 5.12−5.10 (m, 2H), 3.68 (d, 1H, J = 7.2 Hz), 2.9 (d, 1H, J = 6.9 Hz), 1.70 (s, 3H), 1.44 (s, 9H). $[\alpha]_D^{20}$ +56 (*c* 0.65, CH_2Cl_2). ESI-MS: calcd 470.5 $(M + HCO_2H)^+$, found 470.5.

(2*R*,4*S*)-25b: prepared from compound **24** according to the similar procedure as **25a**. Corlorless oil (63%). ^{1}H NMR ($CDCl_3$, 300 MHz): δ ppm 7.40−7.27 (m, 10H), 6.64 (s, 1H), 5.10 (s, 2H), 2.52−2.25 (m, 4H), 1.72 (s, 3H), 1.45 (s, 9H). $[\alpha]_D^{20}$ +50 (*c* 0.30, CH_2Cl_2). ESI-MS: calcd 484.5 $(M + HCO_2H)^+$, found 484.5.

(2*R*,4*S*)-25c: prepared from compound **24** according to the similar procedure as **25a**. Corlorless oil (45%). ^{1}H NMR ($CDCl_3$, 300 MHz): δ ppm 7.40−7.27 (m, 10H), 6.60 (s, 1H), 5.14−5.09 (m, 2H), 2.57−1.53 (m, 9H), 1.45 (s, 9H). $[\alpha]_D^{20}$ + 53.0 (*c* 0.45, $CHCl_3$). EI-MS *m*/*z*: calcd 311 (M^+), found 311.

(*S*)-2-(((9*H*-Fluoren-9-yl)methoxy)carbonylamino)-4-*tert*-butoxy-2-methyl-4-oxobutanoic Acid ((*S*)-27a). To a solution of 5 mmol of oxazolidinone (2*R*,4*S*)-**25a** in 4 mL of MeOH were added 2 equiv of 2 N aqueous NaOH, and the mixture was stirred for 2 h at 45 °C. It was then diluted with 50 mL of water, and the aqueous layer was extracted with Et_2O. The aqueous layer was cooled to 0 °C and the pH adjusted to 3 with 2 N HCl. The acidic aqueous solution was extracted with EtOAc, the organic layers were combined, dried over Na_2SO_4, and evaporated. The residue and Pd/C (10%) 20 mg in 15 mL of dry methylene chloride, were stirred under hydrogen atmosphere until the starting material disappeared. The catalyst was filtered off, and the filtrate was concentrated to afford the crude product. The residue was dissolved in dioxane−10% Na_2CO_3 (15 mL, 1/2) and the solution stirred on an ice bath 10 min prior to addition of Fmoc-Osu (1.710 g, 5 mmol) in dioxane (5 mL) over 30 min. The mixture was allowed to warm to room temperature and stirred overnight. The cream colored suspension was added to a separatory funnel and washed with ether. The aqueous layer was cooled in an ice bath and acidified with 6 N HCl to pH 3. This aqueous solution was ethyl acetate. Ethyl acetate layers were combined, washed with brine, and dried over anhydrous Na_2SO_4. Solvent was removed in vacuo to yield a light-brown, foamy solid. The crude product was loaded onto a silica gel column and eluted with CH_2Cl_2/MeOH = 10/1 to give **27a** as white foam 1.100 g (51.9%). ^{1}H NMR ($CDCl_3$, 300 MHz): δ ppm 7.77 (d, 2H, J = 7.2 Hz), 7.59 (d, 2H, J = 6.6 Hz), 7.43−7.25 (m, 4H), 5.31 (brs, 1H), 3.14−2.92 (dd, 2H, J = 7.2 Hz), 4.82−4.38 (m, 3H), 1.69 (s, 3H), 1.45 (s, 9H). $[\alpha]_D^{20}$ −17 (*c* 0.8, DMF). ESI-MS: calcd 470.5 $(M + HCO_2H)^+$, found 470.5.

(*S*)-2-(((9*H*-Fluoren-9-yl)methoxy)carbonylamino)-5-*tert*-butoxy-2-methyl-5-oxopentanoic Acid ((*S*)-27b). (*S*)-**27b** was prepared from compound **25b** according to a similar procedure as **27a**. White foam (43.0%). ^{1}H NMR ($CDCl_3$, 300 MHz): δ ppm 7.77 (d, 2H, J = 7.2 Hz), 7.59 (d, 2H, J = 6.6 Hz), 7.43−7.25 (m, 4H), 5.31 (brs, 1H), 4.82−4.38 (m, 3H), 2.52−2.25 (m, 4H), 1.72 (s, 3H), 1.45 (s, 9H). $[\alpha]_D^{20}$ −13 (*c* 0.1, DMF). ESI-MS: calcd 484.5 $(M + HCO_2H)^+$, found 484.5.

(*S*)-2-(((9*H*-Fluoren-9-yl)methoxy)carbonylamino)-6-*tert*-butoxy-2-methyl-6-oxohexanoic Acid ((*S*)-27c). (*S*)-**27c** was prepared from compound **25c** according to a similar procedure as **27a**. White foam (47.0%). ^{1}H NMR ($CDCl_3$, 300 MHz): δ ppm 7.77 (d, 2H, J = 7.2 Hz), 7.59 (d, 2H, J = 6.6 Hz), 7.43−7.25 (m, 4H), 5.31 (brs, 1H), 4.82−4.38 (m, 3H), 2.57−1.53 (m, 9H), 1.45 (s, 9H). $[\alpha]_D^{20}$ −4.2 (*c* 1.96, $CHCl_3$). EI-MS *m*/*z*: calcd 453 $(M)^+$, found 453.

(*R*)-2-(((9*H*-Fluoren-9-yl)methoxy)carbonylamino)-6-*tert*-butoxy-2-methyl-6-oxohexanoic Acid ((*S*)-27d). (*S*)-**27d** was prepared from the D-Ala according to a similar procedure as L-Ala to **27a**. White foam (46.5%). ^{1}H NMR ($CDCl_3$, 300 MHz): δ ppm 7.77 (d, 2H, J = 7.5 Hz), 7.61 (d, 2H, J = 7.2 Hz), 7.40 (t, 2H, J = 7.5 Hz), 7.31 (td, 2H, J = 7.5 Hz), 4.37 (m, 2H), 4.22 (t, 1H), 2.22 (m, 2H), 1.68−2.10 (m, 2H), 1.59 (s, 3H), 1.50−1.54 (m, 2H), 1.44 (s, 9H). $[\alpha]_D^{22}$ +3.5 (*c* 1.89, $CHCl_3$). ESI-MS *m*/*z*: calcd 452.2 $(M - H)^+$, found 452.6.

(*S*)-2-(Benzyloxycarbonylamino)propanoic Acid ((*S*)-28). A solution of 2 N NaOH (60 mL, 120 mmol) and benzyloxycarbonyl chloride (18.84 mL, 132 mmol) were added simultaneously dropwise from two separate syringes into L-alanine (10.080 g, 120 mmol) in 2 N NaOH (66 mL, 132 mmol) with magnetic stirring and ice cooling. After approximately 1 h, the mixture was allowed to react at room temperature for another 1 h. After 100 mL of H_2O was added, the mixture was extracted with Et_2O and acidified with 2 N HCl to adjust the pH to 2−3. The product was taken into ether. The latter ether portions were combined, dried (Na_2SO_4), and evaporated in vacuo to give the (*S*)-**28** (4.963 g, 93.2%) as a white solid. ^{1}H NMR ($CDCl_3$, 300 MHz): δ ppm 7.34 (m, 5H), 5.11 (s, 2H), 4.38 (m, 1H), 1.46 (d, 3H, J = 7.2).

(*R*)-2-(Benzyloxycarbonylamino)propanoic Acid ((*R*)-28). (*R*)-**28** was prepared from D-alanine according to a similar procedure as (*S*)-**28**. White solid (92.7%). ^{1}H NMR ($CDCl_3$, 300 MHz): δ ppm 7.34 (m, 5H), 5.12 (s, 2H), 4.42 (m, 1H), 1.46 (d, 3H, J = 7.2).

(2*S*,4*S*)-2-Phenyl-3-(carbobenzyloxy)-4-methyloxazolidin-5-one ((2*S*,4*S*)-29). To a stirred solution of (*S*)-**28** (9.373 g, 31 mmol) and benzaldehyde dimethyl acetal (6.391 g, 45 mmol) in Et_2O (90 mL) was added 33 mL (270 mmol) of $BF_3 \cdot Et_2O$ at −78 °C. The mixture was stirred at −15 °C for 4 days. The reaction mixture was slowly added to ice-cooled, saturated aqueous $NaHCO_3$ (200 mL), and the mixture was stirred for 30 min. After work-up, the separated organic layer was washed with 5% $NaHCO_3$ and H_2O and then dried (Na_2SO_4). The solvent was removed in vacuo. The residue was dissolved in 140 mL of Et_2O/hexane (3/4) for recrystallization and afforded white crystals of (2*S*,4*S*)-**29** (6.934 g, 71.9%). ^{1}H NMR ($CDCl_3$, 300 MHz): δ ppm 7.26−7.41 (m, 10H), 6.64 (s, 1H), 5.11−5.24 (m, 2H), 4.49 (q, 1H, J = 6.6 Hz), 1.58 (d, 3H, J = 7.2 Hz). $[\alpha]_D^{20}$ −27.0 (*c* 0.9, $CHCl_3$).

(2*R*,4*R*)-2-Phenyl-3-(carbobenzyloxy)-4-methyloxazolidin-5-one ((2*R*,4*R*)-29). (2*R*,4*R*)-**29** was prepared from (*R*)-**28** according to a similar procedure as (2*S*,4*S*)-**29**. White crystals in yield of 72.3%. ^{1}H NMR ($CDCl_3$, 300 MHz): δ ppm 7.26−7.41 (m, 10H), 6.64 (s, 1H), 5.11−5.24 (m, 2H), 4.49 (q, 1H, J = 6.6 Hz), 1.58 (d, 3H, J = 7.2 Hz). $[\alpha]_D^{20}$ +26.4 (*c* 1, $CHCl_3$).

(2*S*,4*R*)-Benzyl 4-(4-*tert*-Butoxy-4-oxobutyl)-4-methyl-5-oxo-2-phenyloxazolidine-3carboxylate ((2*S*,4*R*)-30). To a solution of (2*S*,4*S*)-**29** (2.491 g, 8.0 mmol) and *tert*-butyl 4-iodobutanoate (2.593 g, 9.6 mmol) in THF/HMPA = 4:1 (20 mL) was added LiHMDS (12 mL, 12 mmol) in THF slowly under nitrogen at −78 °C, and the slightly yellow solution was stirred at this temperature for 2 h. Saturated NH_4Cl solution was added, and the THF was removed in vacuo. Then Et_2O was added, and the phases were separated. The organic layer was washed with saturated $NaHCO_3$ and saturated aqueous NaCl solutions, respectively. The organic phase was dried over Na_2SO_4 and evaporated. Purification by flash column chromatography gave compound (2*S*,4*R*)-**30** (0.724 g,

20.0%) as a colorless oil. ^{1}H NMR (DMSO-d_6, 400 MHz, 80 °C): δ ppm 7.07−7.43 (m, 10H), 6.60 (s, 1H), 5.02 (m, 2H), 2.28 (m, 1H), 2.13 (m, 2H), 1.80 (m, 1H), 1.67 (s, 3H), 1.45 (m, 2H), 1.41 (s, 9H). $[\alpha]_D^{20}$ −22.0 (*c* 0.22, $CHCl_3$). EI-MS *m*/*z*: calcd 396 (M − *t*-Bu)$^+$, found 396.

(2*R*,4*S*)-Benzyl 4-(4-*tert*-Butoxy-4-oxobutyl)-4-methyl-5-oxo-2-phenyloxazolidine-3carboxylate ((2*R*,4*S*)-30). (2*R*,4*S*)-**30** was prepared from (2*R*,4*R*)-**29** according to a similar procedure as (2*S*,4*R*)-**30**. Colorless oil (23.2%). ^{1}H NMR (DMSO-d_6, 300 MHz): δ ppm 7.07−7.43 (m, 10H), 6.60 (s, 1H), 5.02 (m, 2H), 2.28 (m, 1H), 2.13 (m, 2H), 1.80 (m, 1H), 1.67 (s, 3H), 1.45 (m, 2H), 1.41 (s, 9H). $[\alpha]_D^{22}$ +53.0 (*c* 0.45, $CHCl_3$). EI-MS *m*/*z*: calcd 396 (M − *t*-Bu)$^+$, found 396.

(*R*)-2-(Benzyloxycarbonylamino)-6-*tert*-butoxy-2-methyl-6-oxohexanoic Acid ((*R*)-31)). To a stirred solution of (2*S*, 4*R*)-**30** (630 mg, 1.39 mmol) in THF/H_2O (3:1, 20 mL) was added LiOH·H_2O (146 mg, 3.47 mmol) at 0 °C. The mixture was stirred overnight at 25 °C. After 3 h, 5% $NaHCO_3$ was added to the reaction mixture. The aqueous layer was washed with Et_2O and then acidified to pH 2 using 2 N HC1. The mixture was extracted with Et_2O, and the organic layer was dried (Na_2SO_4). The solvent was removed in vacuo to yield 443 mg (87.3%) of (*R*)-**31** as a colorless oil, which was used directly for the next step without further purification. ^{1}H NMR ($CDCl_3$, 300 MHz): δ ppm 7.34 (s, 10H), 5.09 (s, 2H), 2.22 (m, 2H), 2.00−2.15 (m, 1H), 1.87 (m, 1H), 1.57 (s, 3H), 1.47−1.54 (m,2H), 1.43 (s, 9H). $[\alpha]_D^{20}$ −2.0 (*c* 0.20, $CHCl_3$).

(*S*)-2-(Benzyloxycarbonylamino)-6-*tert*-butoxy-2-methyl-6-oxohexanoic Acid ((*S*)-31)). (S)-**31** was prepared from (2*R*,4*S*)-**30** according to a similar procedure as (*R*)-**31**. Colorless oil (76.1%), used directly for the next step without further purification. ^{1}H NMR ($CDCl_3$, 300 MHz): δ ppm 7.34 (s, 10H) 5.09 (s, 2H), 2.22 (m, 2H), 2.00−2.15 (m, 1H), 1.87 (m, 1H), 1.57 (s, 3H), 1.47−1.54 (m, 2H), 1.43 (s, 9H).

(*R*)-2-(((9*H*-Fluoren-9-yl)methoxy)carbonylamino)-6-*tert*-butoxy-2-methyl-6-oxohexanoic Acid ((*R*)-32). Compound (*R*)-**31** (443 mg, 1.21 mmol) and 10% Pd/C (44 mg) were stirred vigorously for 3 h in MeOH (50 mL) under an atmosphere of H_2. The reaction mixture was then diluted with MeOH (10 mL) and filtered and washed afterward with MeOH (3−10 mL). Concentration of the filtrate under reduced pressure gave the product (275 mg, 98.3%) as a colorless oil.

The crude product (275 mg, 1.19 mmol) was dissolved in the cosolvent of acetone (10 mL) and water (10 mL) and proper amount of K_2CO_3 to adjust the pH to 9−10. Then Fmoc-OSu (491 mg, 1.45 mmol) was added to this solution at room temperature. The mixture was allowed to stir for 5 h and kept at pH 9−10 by adding K_2CO_3. The mixture was then diluted with water and washed with Et_2O. The aqueous layer was acidified with 2 N HCl to pH 2 and extracted with Et_2O. The combined organic layers were dried (Na_2SO_4), and after filtration the solvent was removed. Purification by flash chromatography and elution with CH_2Cl_2/CH_3OH (10/1) gave compound (*R*)-**32** as colorless oil (378 mg, 69.0%). ^{1}H NMR ($CDCl_3$, 300 MHz): δ ppm 7.77 (d, 2H, *J* = 7.5 Hz), 7.61 (d, 2H, *J* = 7.2 Hz), 7.40 (t, 2H, *J* = 7.5 Hz), 7.31 (t, 2H, *J* = 7.5 Hz), 4.37 (m, 2H), 4.22 (t, 1H), 2.22 (m, 2H), 1.68−2.10 (m, 2H), 1.59 (s, 3H), 1.50−1.54 (m, 2H), 1.44 (s, 9H). $[\alpha]_D^{20}$ −4.2 (*c* 1.96, $CHCl_3$). EI-MS *m*/*z*: calcd 453(M)$^+$, found 453.

(*S*)-2-(((9*H*-Fluoren-9-yl)methoxy)carbonylamino)-6-*tert*-butoxy-2-methyl-6-oxohexanoic Acid ((*S*)-32). (*S*)-**32** was prepared from (*S*)-**31** according to the similar procedure as (*R*)-**32**. Colorless oil (53.4%). ^{1}H NMR ($CDCl_3$, 300 MHz): δ ppm 7.77 (d, 2H, *J* = 7.5 Hz), 7.61 (d, 2H, *J* = 7.2 Hz), 7.40 (t, 2H, *J* = 7.5 Hz), 7.31 (td, 2H, *J* = 7.5 Hz), 4.37(m, 2H), 4.22 (t, 1H), 2.22 (m, 2H), 1.68−2.10 (m, 2H), 1.59 (s, 3H), 1.50−1.54 (m, 2H), 1.44 (s, 9H). $[\alpha]_D^{22}$ +3.5 (*c* 1.89, $CHCl_3$). ESI-MS *m*/*z*: calcd 452.2 (M − H)$^-$, found 452.6.

Cyclo-[CH_2-CO-Adi-Leu-Tyr-(α-Me)Asp-Asn-Ava-Cys]-amide (Peptide 1). ESI-MS *m*/*z*: calcd 920.4 (M − H)$^-$, found 920.4. t_R = 15.3 min (10−70% of solvent B in 30 min, purity 99%); t_R = 21.6 min (10−70% of solvent C in 30 min, purity 99%).

Cyclo-[CH_2-CO-Adi-Leu-Tyr-(α-Me)Asp-Asn-Ava-Cys (O)-(R)]-amide (Peptide 2). ESI-MS, *m*/*z*: calcd 936.4 (M + Na)$^+$, found 936.3. t_R = 14.8 min (10−70% of solvent B in 30 min, purity 99%); t_R = 21.1 min (10−70% of solvent C in 30 min, purity 99%).

Cyclo-[CH_2-CO-Adi-Leu-Tyr-(α-Me)Glu-Asn-Ava-Cys]-amide (Peptide 3). ESI-MS *m*/*z*: calcd 958.4 (M + Na)$^+$, found 958.5. t_R = 15.6 min (10−70% of solvent B in 30 min, purity 99%); t_R = 22.0 min (10−70% of solvent C in 30 min, purity 99%).

Cyclo-[CH_2-CO-Adi-Leu-Tyr-(α-Me)Glu-Asn-Ava-Cys (O)-(R)]-amide (Peptide 4). ESI-MS *m*/*z*: calcd 950.4 (M – H)$^-$, found 950.3. t_R = 14.9 min (10−70% of solvent B in 30 min, purity 99%); t_R = 21.7 min (10−70% of solvent C in 30 min, purity 99%).

Cyclo-[CH_2-CO-Adi-Leu-Tyr-(α-Me)Adi-Asn-Ava-Cys]-amide (Peptide 5). ESI-MS *m*/*z*: calcd 948.4 (M − H)$^-$, found 948.4. t_R = 15.7 min (10−70% of solvent B in 30 min, purity 99%); t_R = 22.5 min (10−70% of solvent C in 30 min, purity 100%).

Cyclo-[CH_2-CO-Adi-Leu-Tyr-(α-Me)Adi-Asn-Ava-Cys (O)-(R)]-amide (Peptide 6). ESI-MS *m*/*z*: calcd 964.4 (M − H)$^-$, found 964.2. t_R = 15.7 min (10−70% of solvent B in 30 min, purity 99%); t_R = 21.9 min (10−70% of solvent C in 30 min, purity 100%).

Cyclo-[CH_2-CO-Adi-Leu-Tyr-(D-(α-Me)Glu)-Asn-Ava-Cys]-amide (Peptide 7). ESI-MS, *m*/*z*: calcd 934.4 (M − H)$^-$, found 934.4. t_R = 15.6 min (10−70% of solvent B in 30 min, purity 99%); t_R = 22.0 min (10−70% of solvent C in 30 min, purity 99%).

Cyclo-[CH_2-CO-Adi-Leu-Tyr-(D-(α-Me)Asp)-Asn-Ava-Cys (O)-(R)]-amide (Peptide 8). ESI-MS *m*/*z*: calcd 950.4 (M − H)$^-$, found 950.3. t_R = 14.9 min (10−70% of solvent B in 30 min, purity 99%); t_R = 21.7 min (10−70% of solvent C in 30 min, purity 99%).

Cyclo-[CH_2-CO-Adi-Leu-(3′-NH_2-Tyr)-(α-Me)Glu-Asn-Ava-Cys]-amide (Peptide 9). ESI-MS, *m*/*z*: calcd 949.4 (M − H)$^-$, found 949.3. t_R = 14.3 min (10−70% of solvent B in 30 min, purity 99%); t_R = 20.5 min (10−70% of solvent C in 30 min, purity 98%).

Cyclo-[CH_2-CO-Adi-Leu-(3′-NH_2-Tyr)-(α-Me)Glu-Asn-Ava-Cys (O)-(R)]-amide (Peptide 10). ESI-MS *m*/*z*: calcd 965.4 (M − H)$^-$, found 965.4. t_R = 13.7 min (10−70% of solvent B in 30 min, purity 99%); t_R = 19.8 min (10−70% of solvent C in 30 min, purity 99%).

Cyclo-[CH_2-CO-Gla-Leu-(3′-NH_2-Tyr)-(α-Me)Adi-Asn-Ava-Cys]-amide (Peptide 11). ESI-MS *m*/*z*: calcd 995.4 (M + H)$^+$, found 995.4. t_R = 14.0 min (10−70% of solvent B in 30 min, purity 99%); t_R = 18.3 min (10−70% of solvent C in 30 min, purity 99%).

Cyclo-[CH_2-CO-Gla-Leu-((3′-NH_2)-Tyr)-(α-Me)Adi-Asn-Ava-Cys(O)-(R)]-amide (Peptide 12). ESI-MS *m*/*z*: calcd 1011.4 (M + H)$^+$, found 1011.0. t_R = 13.6 min (10−70% of solvent B in 30 min, purity 99%); t_R = 17.6 min (10−70% of solvent C in 30 min, purity 99%).

H-Gla-Leu-(3′-NH_2-Tyr)-(α-Me)Glu-Asn-amide (Peptide 13). ESI-MS *m*/*z*: calcd 737.3 (M − H)$^-$, found 737.3. t_R = 10.5 min (10−70% of solvent B in 30 min, purity 99%); t_R = 15.2 min (10−70% of solvent C in 30 min, purity 98%).

***N*-Fmoc-Gla-Leu-(3′-NH_2-Tyr)-(α-Me)Glu-Asn-amide (Peptide 14).** ESI-MS *m*/*z*: calcd 961.4 (M + H)$^+$, found 961.5. t_R = 13.7 min (10−70% of solvent B in 30 min, purity 99%); t_R = 18.2 min (10−70% of solvent C in 30 min, purity 98%).

***N*-Fmoc-Adi-Leu-(3′-$CH_2CH_2CO_2H$-Tyr)-Ac6c-Glu-Asn-amide (Peptide 15).** ESI-MS *m*/*z*: calcd 986.4 (M − H)$^-$, found 986.4. t_R = 14.8 min (10−70% of solvent B in 30 min, purity 99%); t_R = 21.7 min (10−70% of solvent C in 30 min, purity 99%).

H-(3′-$CH_2CH_2CO_2H$-Tyr)-(α-Me)Glu-Asn-amide (Peptide 16). ESI-MS *m*/*z*: calcd 508.2 (M − H)$^-$, found 508.2. t_R = 9.8 min (10−70% of solvent B in 30 min, purity 100%); t_R = 13.9 min (10−70% of solvent C in 30 min, purity 98%).

***N*-Fmoc-(3′-$CH_2CH_2CO_2H$-Tyr)-(α-Me)Glu-Asn-amide (Peptide 17).** ESI-MS *m/z:* calcd 732.3 (M + H)$^+$, found 732.4. t_R = 15.2 min (10−70% of solvent B in 30 min, purity 99%); t_R = 22.5 min (10−70% of solvent C in 30 min, purity 98%).

***N*-Fmoc-Adi-Leu-(3′-NH_2-Tyr)-Ac6c-Glu-Asn-amide (Peptide 18).** ESI-MS *m*/*z*: calcd 911.4 (M − H)$^-$, found 911.4. t_R = 17.8 min (10−70% of solvent B in 30 min, purity 99%); t_R = 25.1 min (10−70% of solvent C in 30 min, purity 98%).

***N*-Fmoc-Gla-Leu-(3′-NH_2-Tyr)-Ac6c-Glu-Asn-amide (Peptide 19).** ESI-MS *m/z:* calcd 943.4 $(M - H)^-$, found 942.7. t_R = 13.6 min (10−70% of solvent B in 30 min, purity 99%); t_R = 21.0 min (10−70% of solvent C in 30 min, purity 98%).

***N*-Fmoc-(*R*)-(α-Me)Adi-Leu-Tyr-Ac6c-Asn-amide (Peptide 20).** ESI-MS *m/z*: calcd 912.6 $(M + H)^+$, found 912.6. t_R = 19.25 min (10−90% of solvent B in 26 min, purity 99%); t_R = 21.8 min (10−90% of solvent C in 27 min, purity 98%).

***N*-Fmoc-(*S*)-(α-Me)Adi-Leu-Tyr-Ac6c-Asn-amide (Peptide 21).** ESI-MS *m/z*: calcd 912.6 $(M + H)^+$, found 912.6. t_R = 19.75 min (10−90% of solvent B in 26 min, purity 99%); t_R = 21.6 min. (10−90% of solvent C in 27 min, purity 97%).

***N*-Fmoc-(*R*)-(α-Me)Adi-Leu-(3′-NH_2-Tyr)-Ac6c-Asn-amide (Peptide 22).** ESI-MS *m/z*: calcd 925.5 $(M - H)^-$, found 925.3. t_R = 13.07 min (10−90% of solvent B in 26 min, purity 99%); t_R = 19.7 min (10−90% of solvent C in 27 min, purity 98%).

***N*-Fmoc-(*S*)-(α-Me)Adi-Leu-(3′-NH_2-Tyr)-Ac6c-Asn-amide (Peptide 23).** ESI-MS *m/z*: calcd 949.5 $(M + Na)^+$, found 949.6. t_R = 14.81 min (10−90% of solvent B in 26 min, purity 98%); t_R = 21.7 min (10−90% of solvent C in 27 min, purity 99%).

Acknowledgment. Appreciation is expressed to Prof. Xu Shen and his colleagues of the DDDC at SIMM for the nice assistance in our use of the Biacore 3000 instrument. This work was supported by the funding from Chinese Academy of Sciences (Grants KSCX2-YW-R-20 and KSCX2-YW-R-25) and Ministry of Science and Technology of China (Grant 2004CB518903).

References

(1) Chardin, P.; Cussac, D.; Maignan, S.; Ducruix, A. The Grb2 adaptor. *FEBS Lett.* **1995**, *369*, 47–51.
(2) Lowenstein, E. J.; Daly, R. J.; Batzer, W. L.; Margolis, B.; Lammers, R.; Ulrich, A.; Skolnick, E. Y.; Bar-Sagi, D.; Schlessinger, J. The SH2 and SH3 domain containing protein Grb2 links receptor tyrosine kinases to Ras signalling. *Cell* **1992**, *70*, 431–442.
(3) Rozakis-Adcock, M.; McGlade, J.; Mbamalu, G.; Pelicci, G.; Daly, R.; Li, W.; Batzer, A.; Thomas, S.; Brugge, J.; Pelicci, M. G.; Schlessinger, J.; Pawson, T. Association of the Shc and Grb2/Sem 5 SH2-containing proteins is implicated in activation of the Ras pathway by tyrosine kinases. *Nature* **1992**, *360*, 689–692.
(4) Sastry, L.; Cao, T.; King, C. R. Multiple Grb2-protein complexes in human cancer cells. *Int. J. Cancer* **1997**, *70*, 208–213.
(5) Saucier, C.; Papavasiliou, V.; Palazzo, A.; Naujokas, M. A.; Kremer, R.; Park, M. Use of signal specific receptor tyrosine kinase oncoproteins reveals that pathways downstream from Grb2 or Shc are sufficient for cell transformation and metastasis. *Oncogene* **2002**, *21*, 1800–1811.
(6) Tari, A. M.; Lopez-Berestein, G. Grb2: a pivotal protein in signal transduction. *Semin. Oncol.* **2001**, *28*, 142–147.
(7) Dharmawardana, P. G.; Peruzzi, B.; Giubellino, A.; Burke, T. R.; Bottaro, D. P. Molecular targeting of growth factor receptor-bound 2 (Grb2) as an anti-cancer strategy. *Anti-Cancer Drugs* **2006**, *17*, 13–20.
(8) Feller, S. M.; Lewitzky, M. Potential disease targets for drugs that disrupt protein−protein interactions of Grb2 and Crk family adaptors. *Curr. Pharm. Des.* **2006**, *12*, 529–548.
(9) Soriano, J. V.; Liu, N.; Gao, Y.; Yao, Z.-J.; Ishibashi, T.; Underhill, C.; Burke, T. R., Jr.; Bottaro, D. P. Inhibition of angiogenesis by growth factor receptor bound protein 2-Src homology 2 domain binding antagonists. *Mol. Cancer Ther.* **2004**, *3*, 1289–1299.
(10) Fretz, H.; Furet, P.; Garcia-Echeverria, C.; Rahuel, J.; Schoepfer, J. Structure-based design of compounds inhibiting Grb2-SH2 mediated protein−protein interactions in signal transduction pathways. *Curr. Pharm. Des.* **2000**, *6*, 1777–1796.
(11) Machida, K.; Mayer, B. J. The SH2 domain: versatile signaling module and pharmaceutical target. *Biochim. Biophys. Acta* **2005**, *1747*, 1–25.
(12) Burke, T. R. Development of Grb2 SH2 domain signaling antagonists: a potential new class of antiproliferative agents. *Int. J. Pept. Res. Ther.* **2006**, *12*, 33–48.
(13) Oligino, L.; Lung, F.-D. T.; Sastry, L.; Bigelow, J.; Cao, T.; Curran, M.; Burke, T. R., Jr.; Wang, S.; Krag, D.; Roller, P. P.; King, C. R. Nonphosphorylated peptide ligands for the Grb2 Src homology 2 domain. *J. Biol. Chem.* **1997**, *272*, 29046–29052.
(14) Long, Y.-Q.; Voigt, J. H.; Lung, F.-D. T.; King, C. R.; Roller, P. P. Significant compensatory role of position Y-2 conferring high affinity to non-phosphorylated inhibitors of GRB2-SH2 domain. *Bioorg. Med. Chem. Lett.* **1999**, *9*, 2267–2272.
(15) Li, P.; Zhang, M.; Long, Y.-Q.; Peach, M. L.; Liu, H.; Yang, D.; Nicklaus, M.; Roller, P. P. Potent Grb2-SH2 domain antagonists not relying on phosphotyrosine mimics. *Bioorg. Med. Chem. Lett.* **2003**, *13*, 2173–2177.
(16) Song, Y.-L.; Peach, M. L.; Roller, P. P.; Qiu, S.; Wang, S.; Long, Y.-Q. Discovery of a novel non-phosphorylated pentapeptide motif displaying high affinity for Grb2-SH2 domain by the utilization of 3′-substituted tyrosine derivatives. *J. Med. Chem.* **2006**, *49*, 1585–1596.
(17) Rahuel, J.; Gay, B.; Erdmann, D.; Strauss, A.; GarciaEcheverria, C.; Furet, P.; Caravatti, G.; Fretz, H.; Schoepfer, J.; Grutter, M. G. Structural basis for specificity of Grb2-SH2 revealed by a novel ligand binding mode. *Nat. Struct. Biol.* **1996**, *3*, 586–589.
(18) Ligand residues are numbered relative to the position of phosphotyrosine, or putative phosphotyrosine, which is denoted 0. Positive numbers are used for amino acids C-terminal to phosphotyrosine, and negative numbers are used for amino acids N-terminal to phosphotyrosine. In our case, the consensus sequence for binding to Grb2-SH2 is YXN, in which Y is denoted 0.
(19) Furet, P.; Gay, B.; Caravatti, G.; Garcia-Echeverria, C.; Rahuel, J.; Schoepfer, J.; Fretz, H. Structure-based design and synthesis of high affinity tripeptide ligands of the Grb2-SH2 domain. *J. Med. Chem.* **1998**, *41*, 3442–3449.
(20) Liu, W. Q.; Vidal, M.; Gresh, N.; Rogues, B. P.; Garbay, C. Small peptides containing phosphotyrosine and adjacent alpha mephosphotyrosine or its mimetics as highly potent inhibitors of Grb2 SH2 domain. *J. Med. Chem.* **1999**, *42*, 3737–3741.
(21) Liu, W.-Q.; Vidal, M.; Olszowy, C.; Million, E.; Lenoir, C.; Dhotel, H.; Garbay, C. Structure−activity relationships of small phosphopeptides, inhibitors of Grb2 SH2 domain, and their prodrugs. *J. Med. Chem.* **2004**, *47*, 1223–1233.
(22) Oishi, S.; Karki, R. G.; Kang, S.-U.; Wang, X.; Worthy, K. M.; Bindu, L. K.; Nicklaus, M. C.; Fisher, R. J.; Burke, T. R., Jr. Design and synthesis of conformationally constrained Grb2 SH2 domain binding peptides employing *R*-methylphenylalanyl based phosphotyrosyl mimetics. *J. Med. Chem.* **2005**, *48*, 764–772.
(23) Kang, S.-U.; Choi, W. J.; Oishi, S.; Lee, K.; Karki, R. G.; Worthy, K. M.; Bindu, L. K.; Nicklaus, M. C.; Fisher, R. J.; Burke, T. R., Jr. Examination of acylated 4-amino piperidine-4-carboxylic acid residues in the phosphotyrosyl+1 position of Grb2 SH2 domain-binding tripeptides. *J. Med. Chem.* **2007**, *50*, 1978–1982.
(24) Shi, Y.-H; Song, Y.-L.; Lin, D.-H.; Tan, J.; Roller, R. P.; Li, Q.; Long, Y.-Q.; Long, Y.-Q.; Song, G.-Q. Binding affinity difference induced by the stereochemistry of the sulfoxide bridge of the cyclic peptide inhibitors of Grb2-SH2 domain: NMR studies for the structural origin. *Biochem. Biophys. Res. Commun.* **2005**, *330*, 1254–1261.
(25) Long, Y.-Q.; Lung, F.-D. T.; Roller, P. P. Global optimization of conformational constraint on non-phosphorylated cyclic peptide antagonists of the Grb2-SH2 domain. *Bioorg. Med. Chem.* **2003**, *11*, 3929–3936.
(26) Roller, P. P.; Long, Y.-Q.; Lung, F.-D.T.; Voigt, J. H.; King, C. R. *Peptides 1998*, Proceedings of the 25th European Peptide Symposium; Bajusz, S., Hudecz, F., Eds.; Akademiai Kiado: Budapest, Hungary, 1999; pp 706−707.
(27) Altman, E.; Nebel, K.; Mutter, M. Versatile stereoselective synthesis of completely protected trifunctional α-methylated α-amino acids starting from alanine. *Helv. Chim. Acta* **1991**, *74*, 800–806.
(28) Song, Y.-L; Tan, J.-Z.; Luo, X.-M.; Long, Y.-Q. Utilization of 3′-carboxy containing tyrosine derivatives as a new class of phosphotyrosyl mimetics in the preparation of novel non-phosphorylated cyclic peptide inhibitors of Grb2-SH2 domain. *Org. Biomol. Chem.* **2006**, *4*, 659–666.
(29) Karady, S.; Amato, J. S.; Weinstock, L. M. Enantioretentive alkylation of acyclic amino acids. *Tetrahedron Lett.* **1984**, *25*, 4337–4340.
(30) Song, Y.-L.; Roller, P. P.; Long, Y.-Q. Development of L-3-aminotyrosine suitably protected for the synthesis of a novel non-phosphorylated hexapeptide with low-nanomolar Grb2-SH2 domain-binding affinity. *Bioorg. Med. Chem. Lett.* **2004**, *14*, 3205–3208.
(31) Furet, P.; Gay, B.; Garcia-Echeverria, C.; Rahuel, J.; Fretz, H.; Schoepfer, J.; Caravatti, G. Discovery of 3-amino-benzyloxycarbonyl as N-terminal group inimal phosphopeptide sequence recognized by the Grb2-SH2 domain. *J. Med. Chem.* **1997**, *40*, 3551–3556.
(32) Rahuel, J.; Garcia-Echeverria, C.; Furet, P.; Strauss, A.; Caravatti, G.; Fretz, H.; Schoepfer, J.; Gay, B. Structural basis for the high affinity of amino-aromatic SH2 phosphopeptide ligands. *J. Mol. Biol.* **1998**, *279*, 1013–1022.
(33) Garcia-Echeverria, C.; Furet, P.; Gay, B.; Fretz, H.; Rahuel, J.; Schoepfer, J.; Caravatti, G. Potent antagonists of the SH2 domain of Grb2: optimization of the X+1 position of 3-amino-*Z*-Tyr(PO_3H_2)-X+1-Asn-NH_2. *J. Med. Chem.* **1998**, *41*, 1741–1744.

JM800487R